

# Anisotropy in the wet-etching of semiconductors

John J. Kelly \*, Harold G.G. Philipsen

*Debye Institute, Condensed Matter and Interfaces, Utrecht University, P.O. Box 80000, 3508 TA Utrecht, The Netherlands*

---

## Abstract

The surface chemistry and electrochemistry of the anisotropic etching of semiconductors are reviewed. Recent insights into the anisotropic chemical etching of silicon in alkaline solution and of electrochemical etching of anisotropic pores in n-type semiconductors are described. The possible role of galvanic effects in open-circuit etching is emphasized.

© 2006 Published by Elsevier Ltd.

*Keywords:* Wet-etching; Silicon; III–V Semiconductors; Electrochemistry; Galvanic effects

---

## 0. Introduction

Because of simplicity, cost-effectiveness and versatility, wet-chemical etching methods find wide application in semiconductor device technology. While some semiconductors can be decomposed by reduction, practical etching generally involves oxidation of the solid [1]. Valence electrons are removed from surface bonds to an etching species in solution (open-circuit etching) or to a counter electrode via an external circuit (electrochemical etching). For open-circuit etching one can distinguish two mechanisms. The first is ‘electrochemical’: an oxidizing agent in solution extracts bonding electrons from the valence band of the solid, i.e., it ‘injects holes’ which, when localized at the surface, cause bond rupture. Since holes are mobile carriers, the two reactions – reduction of the oxidizing agent and oxidation of the solid – can be considered as independent electrochemical reactions; they can be spatially separated (an example of this will be given below). This form of etching is generally referred to as *electroless*. The second mechanism is *chemical*: an electron-exchange reaction occurs directly between the active etching agent in solution and surface atoms. Bonds in the etching agent and solid are

broken and new bonds are formed in a localized and synchronous reaction, not involving free holes.

Two main parameters can determine the rate of etching of the semiconductor: the kinetics of the surface reaction(s) or mass transport of reactants or products in solution. If the surface reaction is fast then etching will be determined by the hydrodynamics of the system and the etch rate will not be sensitive to the nature of the surface, e.g., its crystallographic orientation or morphology. Mass-transport determined etching, being isotropic, gives rise to rounded profiles at mask edges. On the other hand, if surface kinetics are important, then the etch rate is very likely to be sensitive to surface orientation. Different crystal faces may dissolve at different rates; etching at a mask edge is anisotropic and will reveal slow-etching facets. Clearly, both forms of etching are interesting for making devices and have found wide application in optoelectronics technology.

Since open-circuit etching does not require an electrochemical cell and voltage source, it is more attractive for many applications. Both chemical and electroless methods have made a considerable contribution to the development of III–V optoelectronics [1,2]. Chemical etchants are, in general, more likely to be anisotropic (see below). Microelectromechanical systems (MEMS) technology relies heavily on the anisotropic etching of silicon in alkaline solution [3]. Despite the fact that the technologists continue to dazzle us with their feats, the chemistry of this system is still not well understood. In Section 1 some new insights and

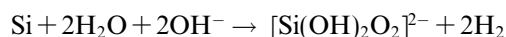
---

\* Corresponding author. Tel.: +31 30 253 2220; fax: +31 30 253 2403.  
E-mail address: [j.j.kelly@phys.uu.nl](mailto:j.j.kelly@phys.uu.nl) (J.J. Kelly).

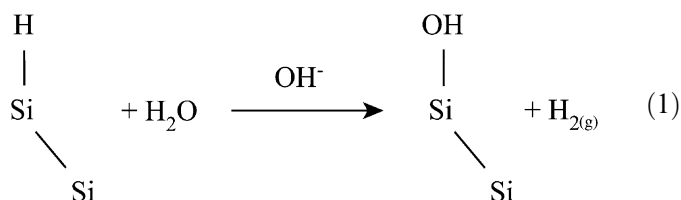
models will be presented. Even when electroless etching is mass-transport controlled, unexpected anisotropy may turn up (this has been known for a long time and, though important, is generally ignored). In Section 2 we show how such anisotropy can be understood on the basis of galvanic interaction between etching facets. We also consider possible consequences for chemical etching systems. In the final section we describe recent developments in a special field: anisotropic porous materials; electrochemical etching is used to make ordered and highly oriented pores in semiconductors. Such materials will be important for applications in photonics.

### 1. Chemical etching: silicon in alkaline solution

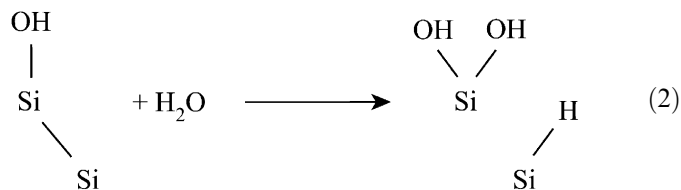
Dissolution of InP in concentrated HCl solution or of Si in alkaline solution are examples of chemical etching showing strong anisotropy [1,4,\*5,\*6]. The Si reaction can be represented globally by [7]



Although this clearly is a complex multi-step reaction there is general agreement that two reaction steps are important [\*5,\*8,\*9,10,11]. Removal of the native oxide from Si leaves the surface hydrogen-terminated [12]. The first etching step involves nucleophilic attack by an  $\text{OH}^-$  ion on the Si–H surface bond.



The activated state of this reaction is a pentacoordinated Si atom [13]. The departing ‘hydride’ reacts with  $\text{H}_2\text{O}$  to give hydrogen gas and the surface atom is hydroxylated. The presence of the OH group at the surface polarizes the Si–Si back bond (only one of these is shown). The bond is attacked by water with the OH adding to the positively polarized surface atom and H to the sub-surface atom.



In this way hydrogen termination of the surface is restored. Whether the surface is hydrogenated (hydrophobic) or hydroxylated (hydrophilic) during etching will depend on the relative rates of reactions (1) and (2).

The reactivity of the surface is determined by the kinetics of reactions of this type. To start, we consider ideal, i.e., atomically flat, (100) and (111) surfaces. In the (100) case each surface atom has a dihydride termination and is

bonded to two sub-surface Si atoms. In the (111) case the surface is monohydride terminated with three back bonds. These differences have important consequences for the reactivity. The dihydride is chemically less stable than the monohydride (it is easier to form the pentavalent intermediate), indicating that the rate of reaction (1) should be faster for the (100) surface [13]. Since it should be easier to dislodge a (100) Si atom with only two back bonds, the rate of reaction (2) should also be faster than that for the (111) surface. This naïve reasoning can explain the very large difference in etch rates for the two surfaces (this can be more than two orders of magnitude). However, surfaces are seldom ideal. For example, under etching conditions the (111) surface consists of atomically flat hydrogen-terminated terraces defined by atomic steps. (The (100) surface is not atomically flat under similar conditions.) Since coordination of the Si atom to the lattice is lower at step edges and kink sites it is much easier to remove the atom than from a terrace site. Consequently, etching occurs by a step-flow mechanism. This has been revealed in the in situ STM studies of Allongue et al. [\*14] while the hydrogen termination is clear from both ex situ and in situ infrared spectroscopy [\*8,15]. The high stability of the (111) terraces is also clear from the slow kinetics of anodic oxidation of n-type material; the electrochemical reaction depends on the (slow) chemical attack on the surface [10].

By comparing STM images of (111) surfaces etched under mild conditions ( $\text{HF}/\text{NH}_4\text{F}$  solution at  $\text{pH} \geq 8$ ) with morphologies predicted with kinetic Monte Carlo simulations, Hines was able to determine the relative reactivities of the various sites on the surface [16]. In subsequent work [\*5,\*6] this group used an elegant ‘orientation-resolved’ approach to study site reactivity in the etching of Si in KOH solution. This involved micromachined test patterns on Si(110) wafers. Such wagon-wheel patterns (see Fig. 1) allow one in a single experiment to study both etch rate and surface morphology of a whole range of surfaces that differ only in their miscut. The results of this work, which included the influence of  $\text{OH}^-$  concentration and temperature as well as isotope effects, were surprising. While the authors found no evidence for a change in chemical mechanism with surface orientation (they consider reaction (1) to be rate determining), transitions between rough and smooth etch morphologies were found at the same orientations at which etch rate discontinuities occur (see Fig. 2). The origin of such morphological transitions is unclear. The authors conclude that the complexity of the phenomena is due to the multi-site nature of the etching reaction.

The most sophisticated approach to modelling of the wet chemical etching of Si can be found in the thesis of Erik van Veenendaal [17] and in publications by him and co-workers. By introducing new concepts to a continuum description they obtained analytical expressions for crystal growth and etch rates as a function of crystallographic orientation [18]. These network functions contain a limited number of physically meaningful variables. The function

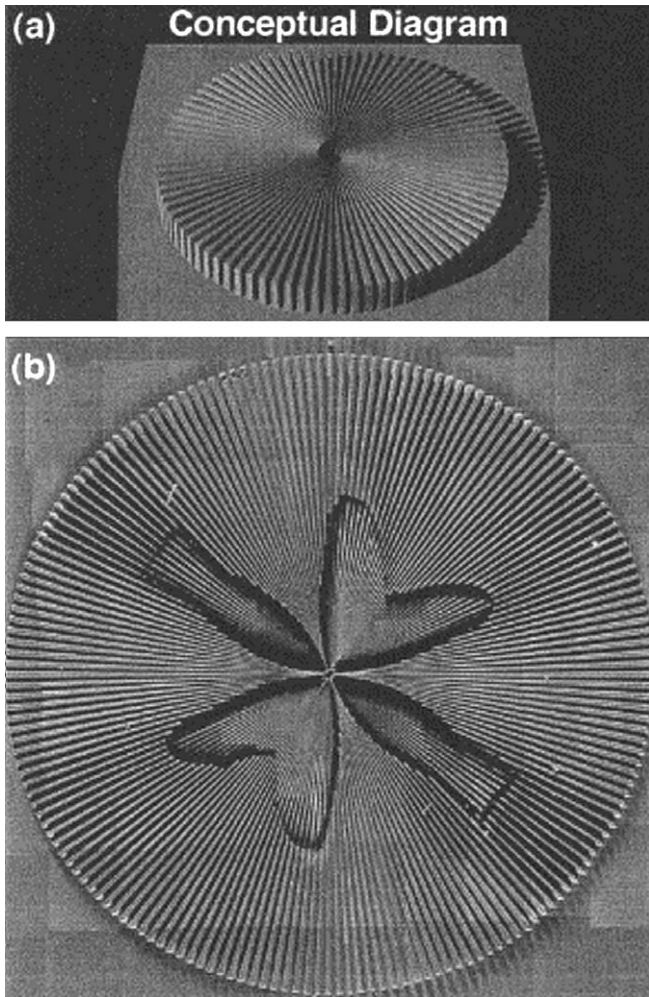


Fig. 1. The micromachined wagon-wheel pattern (a) conceptual diagram and (b) optical micrograph of etched pattern. The pattern is 16 mm in diameter and each wedge is 1° wide. (From Ref. [\*6].)

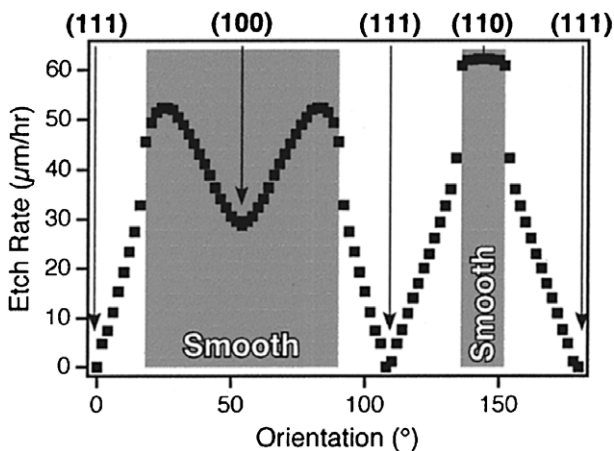


Fig. 2. Etch rate as a function of crystallographic orientation, determined using the microfabricated wagon-wheel. The transition between rough and smooth etch morphologies occurs at the same orientation as the etch rate discontinuities. Conditions: 70 °C, 50% KOH. (From Ref. [\*5].)

formulated for wet-chemical etching of Si in KOH reproduces the essential features of the experimental results

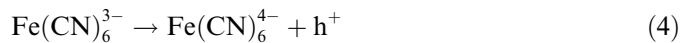
obtained with hemispherical samples [19]. In addition, an atomistic approach using Monte Carlo simulation was used to explain the occurrence of protrusions on etched Si(100) and Si(110) surfaces and to study kinetic roughening [20]. Finally, the group developed two different tools for continuum simulation of crystal shape evolution during etching.

## 2. Electroless etching: galvanic effects

In electroless etching two electrochemical reactions occur [\*21]. For the oxidation (and dissolution) of the solid electrons must be removed from surface bonds, i.e., valence band holes are required at the interface with the solution. For example, in the case of a III–V semiconductor such as GaAs, six holes are generally needed to dissolve one formula unit. In alkaline solution the reaction can be represented by



A strong oxidizing agent such as the ferricyanide ion in solution can extract electrons from the valence band of the semiconductor; this is equivalent to the ‘injection’ of holes into the band;



If holes are localized in surface bonds then the solid is oxidized (reaction (3)).

The rate of electroless etching (reactions (3) and (4)) can depend on mass transport in solution in two ways, via diffusion of  $\text{OH}^-$  ions (reaction (3)) or of the oxidizing agent (reaction (4)). In both cases the kinetics of the reactions at the GaAs surface are fast. For individual faces the etch rate is diffusion controlled and independent of the face. On this basis one would expect isotropic etching at mask edges. This is the case for  $\text{OH}^-$  controlled dissolution. However, for the case in which  $\text{Fe}(\text{CN})_6^{3-}$  transport controls etching, facets develop at resist edges (see SEM cross sections, Fig. 3). This result is also observed with other ‘hole-injecting’ oxidizing agents.

This surprising difference in etching properties can be understood on the basis of the electrochemistry of electroless etching. At high  $\text{OH}^-$  concentration, the rate of the oxidation (reaction (3)) depends on the hole concentration at the surface. Consequently, for a p-type electrode the anodic oxidation current ( $i$ ) increases exponentially as the potential ( $V$ ) is made positive. This is shown schematically in Fig. 3 for two crystal faces of GaAs. The more stable (111) Ga face (case A) is oxidized at a more positive potential than the more reactive (100) face (case B). The reaction involving hole injection from the oxidizing agent in solution into the valence band of the semiconductor (reaction (4)) is diffusion controlled, i.e., the cathodic reduction current is independent of the potential in a broad range (case A and B in Fig. 3). For open-circuit etching in the steady state the rates of oxidation and reduction must be equal. This condition defines the open-circuit potential,  $V_A$  and

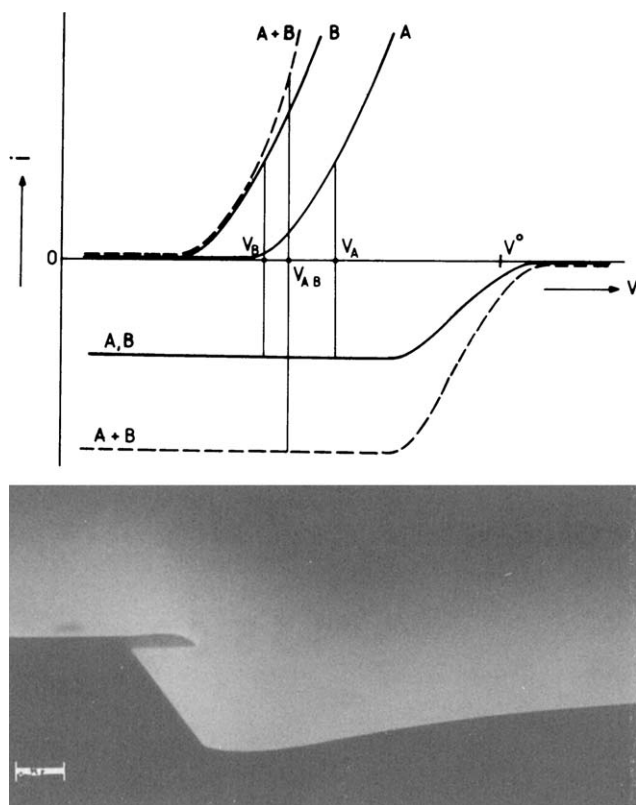


Fig. 3. Current–potential ( $i$ – $V$ ) curves showing galvanic element formation between two crystal faces, A and B. Etching is controlled by diffusion of the oxidizing agent. The inset shows the corresponding faceted profile. (From Ref. [\*21].)

$V_B$  for the A and B faces, respectively. In both cases the semiconductor is etched at the same rate, controlled by mass transport of the oxidizing agent.

When the two surfaces are brought into electrical contact, it is necessary to consider the total anodic and total cathodic current–potential curves (A + B, dashed lines, Fig. 3). The new rest potential  $V_{AB}$  lies between the values for the individual surfaces. Since  $V_{AB}$  is negative with respect to  $V_A$  and positive with respect to  $V_B$ , the etch rate of the more stable surface is diminished while that of the reactive surface is enhanced. In fact, holes supplied to the A face are used to etch preferentially the B face; a galvanic cell is formed. This model can therefore explain why a faceted profile is obtained even though the individual free surfaces are etched at a diffusion-controlled rate (see inset of Fig. 3).

In Fig. 4 corresponding to the case in which the  $\text{OH}^-$  concentration is low (lower than that of the oxidizing agent) the situation is reversed. The anodic reaction is now mass-transport limited (by diffusion of  $\text{OH}^-$  ions). The difference in reactivity between the A and B faces is again clear from the anodic current onset. On the basis of this figure one can conclude that, because the anodic current is potential independent, the etch rates of the A and B faces are not affected when the two surfaces are connected electrically (A + B case). It is clear that in this case

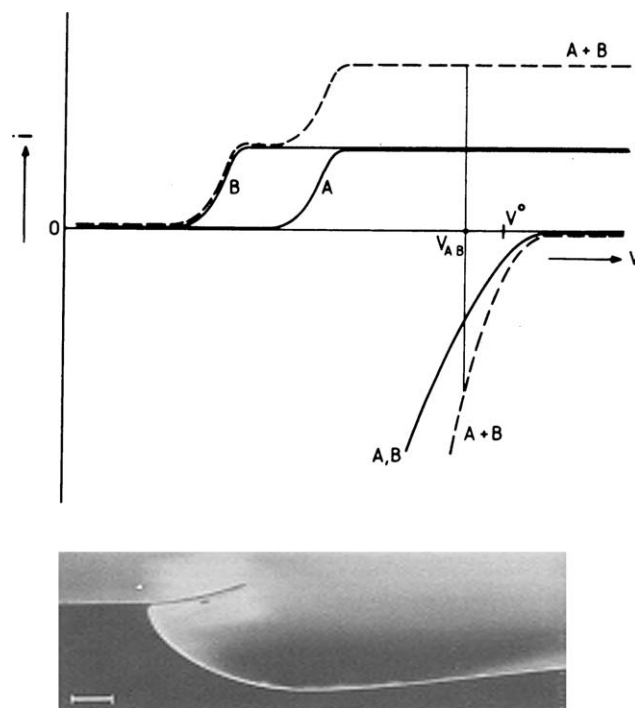


Fig. 4. As for Fig. 3 but etching is controlled by the anodic reaction ( $\text{OH}^-$  diffusion) and a rounded profile is obtained. (From Ref. [\*21].)

the more stable surface is not ‘protected’. In fact, all surfaces are dissolved at the same rate, which is determined by  $\text{OH}^-$  diffusion. Etching at resist edges is expected to be isotropic (see inset of Fig. 4).

Free holes are not involved in a chemical etching reaction such as that of Si in alkaline solution. Consequently, galvanic interaction of the type described above for electroless etching of GaAs is not expected. Previous work has shown, however, that the chemical etch rate is sensitive to the electrochemical potential of the Si [11]. This is particularly the case for the n-type semiconductor where the etch rate in KOH solution is reduced markedly at negative potential. This effect can be attributed to the influence of the potential drop in the Helmholtz layer (at the solid–solution interface) on ion- and electron-transfer reactions such as (1) and (2). Under chemical etching conditions the open-circuit potential of Si, which is determined by anodic oxidation of the solid and cathodic reduction of water, differs for the different faces of the semiconductor [22]. This is clear when a V-groove is etched in a (100) wafer to expose (111) facets. The open-circuit potential changes by as much as 200 mV. Such changes can alter the etch rates of the individual facets and thus the anisotropy of the system [23]. Raisch et al. used an explanation based on galvanic interaction between (100) and (111) faces to explain the stability of micropyramids formed on (100) surfaces during anisotropic etching [24]. The importance of galvanic effects in Si etching was first pointed out by Allongue et al. [25]; they showed that cathodic protection of the polished surface of a (111) Si wafer by a roughened back surface helps to promote the formation of ideally flat

hydride-terminated (111) surfaces. It is clear that, despite the *chemical* nature of anisotropic etching reactions, *electrochemical* factors should not be disregarded.

### 3. Anodic etching: anisotropic pores

Porous anodic etching of Si in HF solution has been known and applied for many years [26,\*\*27]. A particularly interesting aspect is the etching of highly ordered and strongly anisotropic mesopores and macropores with dimensions in the range  $<50$  nm and  $\geq 50$  nm, respectively. In n-type Si such pores can be grown by photoanodic etching, an approach perfected by Lehmann et al. [\*\*27]. To define the two-dimensional ordering, a pattern of etch pits is introduced onto the front side of the Si surface by, for example, photolithography and anisotropic chemical etching (see Fig. 5).

The wafer is illuminated from the back side. The photo-generated holes are collected at the front side at the tips of the etch pits where the electric field of the depletion layer is strongest (the electrons pass to the counter electrode and are registered in the external circuit). Preferential dissolution at the tips gives rise to pores which grow in crystallographically favoured directions,  $\langle 100 \rangle$ -oriented pores in the case of (100)Si. The pore dimensions depend on the donor density and the etching conditions. By modulating both the light intensity and applied potential during etching, Gösele and co-workers [\*\*28] have recently succeeded in extending this approach from two to three dimensions (see Fig. 6). Subsequent anisotropic etching in alkaline solution allowed them to modulate further these porous structures. In recent work [29] Lehmann has shown that

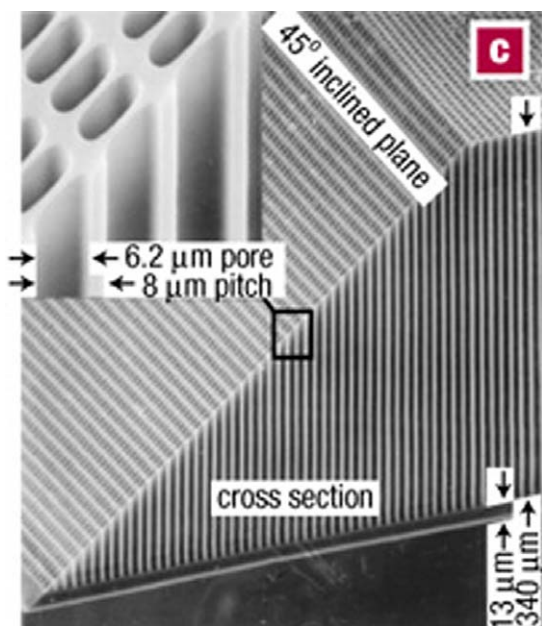


Fig. 5. SEM micrograph of macroporous n-type silicon. The pore positions are defined photolithographically before anodization.

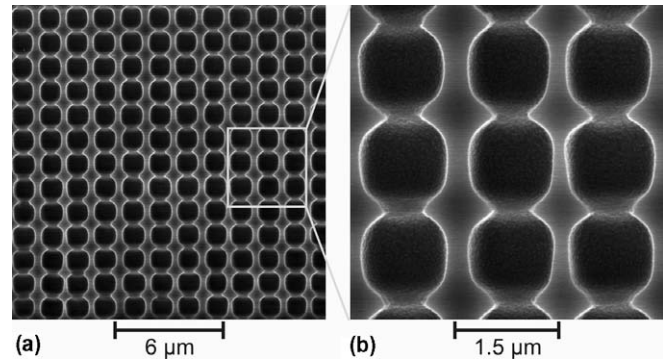


Fig. 6. SEM micrographs of strongly modulated porous n-type Si. Part (a) shows an overview and (b) a close-up. (From Ref. [\*\*28].)

square pore cross sections and pore arrays of high porosity can be produced by subsequent alkaline etching of macroporous Si membranes. By the proper choice of etchant the rounded pore walls can be etched to reveal either (100) or (110) faces.

Etching of anisotropic pores by the photoanodic approach is made possible in Si by the large diffusion length of the holes (they can cross the wafer from the back side to the pore fronts at the other side). Because of a much smaller minority carrier diffusion length the photoanodic approach is not applicable to other semiconductors. Instead, holes can be generated by applying a strongly positive potential to an n-type semiconductor in the dark to induce electrical breakdown. In this case the band bending at the surface is such that electrons can tunnel from the top of the valence band to the conduction band, leaving holes in the valence bands. Etching is localized; it occurs where the electric field is strongest and pores are formed. The strong electric field at the pore fronts (due to the curvature) again ensures propagation of the pores. This mechanism is supported by the observation of light emission from the pore fronts during etching of n-type GaP [30,34]. In this case electroluminescence is caused by impact ionization resulting from the injection of hot electrons into the conduction band.

Among the first examples of strong anisotropy in porous etching of a semiconductor other than Si was that reported by Takizawa et al. who produced pores with an aspect ratio larger than 100 in  $\langle 111 \rangle$  A-oriented n-type InP in HCl solution [31]. By prestructuring the surface using a mask they were able to fabricate a high density, highly ordered two-dimensional pore pattern. Such work has been extended to other semiconductors such as GaAs [\*\*32] and more recently to GaP [33,34]. The primary pores in (100) GaAs grow in the  $\langle 111 \rangle$  B-direction, in contrast to Si where the pores grow in the  $\langle 100 \rangle$  and  $\langle 113 \rangle$  directions. Ross et al. were among the first to develop a model to account for such differences [35]. Their model is based on two assumptions: first, etching occurs at sharply curved pore fronts where the electric field is strongest; second, atoms are removed preferentially from surface kink sites, where reactivity is higher because of the lower coordination

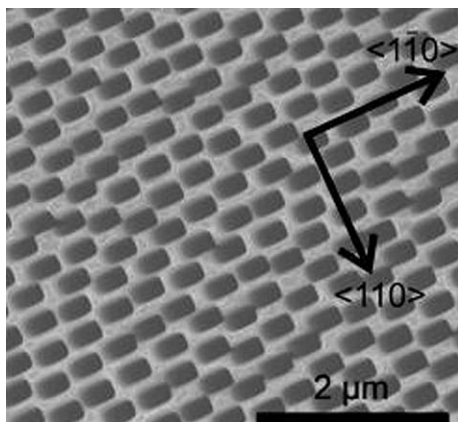


Fig. 7. Top view of a self-organized array of rectangular pores in (100)-oriented n-type GaP. The vectors indicate the crystallographic directions. (From Ref. [\*\*32].)

to the lattice. With this model the pore shapes could be understood as well as the basic differences between the two semiconductors.

Föll et al. have provided an extensive review of pore formation in III–V semiconductors and have compared these compound semiconductors with Si [\*\*32]. They distinguish two main factors determining the growth direction of anisotropic pores.

- (1) Pores may be crystallographically oriented. The only growth direction reflecting crystal structure in III–V semiconductors is  $\langle 111 \rangle_B$ , where B refers to the group V element. In Si two crystallographic pore directions –  $\langle 100 \rangle$  and  $\langle 113 \rangle$  – are found. Pores in Si never grow in the  $\langle 111 \rangle$  direction for reasons discussed in Section 1.
- (2) Alternatively, pores may follow the flow of current, their orientation being normal to the equipotential surfaces in the wafer. Current-line-oriented pores are therefore perpendicular to the surface except at, for example, mask edges where they tend to curve.

It is clear that anodic anisotropic porous etching is even more complex than anisotropic chemical etching. Apart from crystallographically determined surface chemistry, factors such as the local electric field, surface passivation and mass transport in solution are important. Very often the initial pore nucleation plays an essential role [36]. There are a number of examples of self-organization of pores [\*\*32,33]. Synchronized and unsynchronized oscillations in pore dimensions are coupled to current and voltage oscillations. Föll et al. conclude that ‘many features are still awaiting discovery, not to mention explanation’. Subsequent results by Schmuki et al. with GaP confirm the wisdom of this conclusion [33]. They found surprisingly that by replacing the widely used  $H_2SO_4$  or HF electrolyte solutions by a HBr solution the pore morphology changes drastically. Whereas the former solution gives a random (isotropic) porous structure, HBr results in well-defined

micron-long rectangular pores in GaP. The etched channels grow perpendicular to the (100) surface; they show an etch stop at the (110) planes and give a self-organized structure (see Fig. 7). It is not clear why the change of electrolyte has such a dramatic effect on pore growth.

#### 4. Conclusions

Anisotropic etching in its various forms is widely applied in device fabrication. The mechanisms of such processes are extremely complex, involving a broad variety of physical and chemical factors. While these factors are known, our current models are, in general, not able to explain many of the subtleties observed experimentally. This holds for both anisotropic chemical and meso/macro-porous etching.

#### References

The papers of particular interest have been highlighted as:

- \* of special interest;
- \*\* of very special interest.

- [1] Notten PHL, Van den Meerakker JEAM, Kelly JJ. Etching of III–V semiconductors: an electrochemical approach. Oxford: Elsevier; 1991.
- [2] Pearton SJ, Ren F. Wet chemical etching of compound semiconductors. *Electrochem Soc Proc* 2005;PV2005-04:147–59.
- [3] Elwenspoek M, Jansen H. In: *Silicon micromachining, Cambridge studies in semiconductor physics and microelectronic engineering*, vol. 7, 1998.
- [4] Wang J, Thompson DA, Simmons JG. Wet chemical etching for V-grooves into InP substrates. *J Electrochem Soc* 1998;145(8):2931–7.
- [\*5] Wind RA, Jones H, Little MJ, Hines MA. Orientation-resolved chemical kinetics: using microfabrication to unravel the complicated chemistry of KOH/Si etching. *J Phys Chem B* 2002;106(7):1557–69.
- [\*6] Wind RA, Hines MA. Macroscopic etch anisotropies and microscopic reaction mechanisms: a micromachined structure for the rapid assay of etchant anisotropy. *Surf Sci* 2000;460(1–3):21–38.
- [7] Seidel H, Csepregi L, Heuberger A, Baumgärtel H. Anisotropic etching of crystalline silicon in alkaline solutions – I – Orientation dependence and behavior of passivation layers. *J Electrochem Soc* 1990;137(11):3612–26.
- [\*\*8] Raisch P, Haiss W, Nichols RJ, Schiffrin DJ. Time domain impedance spectroscopy for probing the termination of silicon (100) surfaces in aqueous solution. *J Phys Chem B* 2001;105(50):12508–15.
- [\*9] Allongue P, Costa-Kieling V, Gerischer H. Etching of silicon in NaOH solutions – II – Electrochemical studies of n-Si(111) and (100) and mechanisms of the dissolution. *J Electrochem Soc* 1993;140(4):1018–26.
- [10] Philipsen HGG, Kelly JJ. Anisotropy in the anodic oxidation of silicon in KOH solution. *J Phys Chem B* 2005;109(36):17245–53.
- [11] Xia XH, Kelly JJ. Chemical etching and anodic oxidation of (100) silicon in alkaline solution: the role of applied potential. *Phys Chem Chem Phys* 2001;3(23):5304–10.
- [12] (a) Gräf D, Grundner M, Schulz R. Reaction of water with hydrofluoric acid treated silicon(111) and (100) surfaces. *J Vac Sci Technol A* 1989;7(3):808–13;  
(b) Angermann H, Henrion W, Rebien M, Zettler J-T, Röseler A. Characterization of chemically prepared Si-surfaces by UV–VIS and

- IR spectroscopic ellipsometry and surface photovoltage. *Surf Sci* 1997;388:15–23;
- (c) Dumas P, Chabal YJ, Jakob P. Morphology of hydrogen-terminated Si(111) and Si(100) surfaces upon etching in HF and buffered-HF solutions. *Surf Sci* 1992;269/270:867–73.
- [13] Baum T, Schiffrin DJ. Mechanistic aspects of anisotropic dissolution of materials: etching of single-crystal silicon in alkaline solutions. *J Chem Soc – Far Trans* 1998;94(5):691–4.
- [\*14] Allongue P, Costa-Kieling V, Gerischer H. Etching of silicon in NaOH solutions – I – In situ scanning tunneling microscopy investigation of n-Si(111). *J Electrochem Soc* 1993;140(4):1009–18.
- [15] Haiss W, Raisch P, Schiffrin DJ, Bitsch L, Nichols RJ. An FTIR study of the surface chemistry of the dynamic Si(100) surface during etching in alkaline solution. *Faraday Discuss* 2002;121:167–80.
- [16] Hines MA. The picture tells the story: using surface morphology to probe chemical etching reactions. *Int Rev Phys Chem* 2001;20(4):645–72.
- [17] van Veenendaal E. From an atomistic to a continuum description of crystal growth – application to wet chemical etching of silicon. PhD thesis. Katholieke Universiteit Nijmegen, The Netherlands, 2001.
- [18] (a) van Suchtelen J, van Veenendaal E. The construction of orientation-dependent crystal growth and etch rate functions – Part I – Mathematical and physical aspects. *J Appl Phys* 2000;87(12):8721–31;
- (b) van Veenendaal E, van Suchtelen J, van Enkevort WPJ, Sato K, Nijdam AJ, Gardeniers JGE, et al. The construction of orientation-dependent crystal growth and etch rate functions – Part II – Application to wet chemical etching of silicon in potassium hydroxide. *J Appl Phys* 2000;87(12):8732–40.
- [19] van Veenendaal E, Sato K, Shikida M, van Suchtelen J. Micromorphology of single crystalline silicon surfaces during anisotropic wet chemical etching in KOH and TMAH. *Sens Actuators A* 2001;93(3):219–31.
- [20] van Veenendaal E, Sato K, Shikida M, Nijdam AJ, van Suchtelen J. Micro-morphology of single crystalline silicon surfaces during anisotropic wet chemical etching in KOH: velocity source forests. *Sens Actuators A* 2001;93(3):232–42.
- [\*21] Notten PHL, Kelly JJ. Evidence for cathodic protection of crystallographic facets from GaAs etching profiles. *J Electrochem Soc* 1987;134(2):444–8.
- [22] Smith RL, Kloeck B, De Rooij N, Collins SD. The potential dependence of silicon anisotropic etching in KOH at 60 °C. *J Electroanal Chem* 1987;238:103–13.
- [23] Kretschmer H-R, Xia XH, Kelly JJ, Steckenborn A. Anisotropic etching of three-dimensional shapes in silicon: the important role of galvanic interaction. *J Electrochem Soc* 2004;151(10):C633–6.
- [24] Raisch P, Haiss W, Nichols RJ, Schiffrin DJ. In-situ atomic force microscopy of silicon(100) in aqueous potassium hydroxide. *Electrochim Acta* 2000;45(28):4635–43.
- [25] Allongue P, Henry de Villeneuve C, Morin S, Boukherroub R, Wayner DDM. The preparation of flat H–Si(111) surfaces in 40% NH<sub>4</sub>F revisited. *Electrochim Acta* 2000;45(28):4591–8.
- [26] Lehmann V. *Electrochemistry of silicon – instrumentation, science, materials and applications*. Weinheim: Wiley-VCH; 2002.
- [\*\*27] (a) Lehmann V. The physics of macropore formation in low doped n-type silicon. *J Electrochem Soc* 1993;140(10):2836–43;
- (b) Lehmann V, Ronnebeck S. The physics of macropore formation in low-doped p-type silicon. *J Electrochem Soc* 1999;146(8):2968–75;
- (c) Ottow S, Lehmann V, Föll H. Processing of three-dimensional microstructures using macroporous n-type silicon. *J Electrochem Soc* 1996;143(1):385–90.
- [\*\*28] (a) Matthias S, Müller F, Gösele U. Simple cubic three-dimensional photonic crystal based on macroporous silicon and anisotropic posttreatment. *J Appl Phys* 2005;98:023524;
- (b) Matthias S, Müller F, Schilling J, Gösele U. Pushing the limits of macroporous silicon etching. *Appl Phys A* 2005;80(7):1391–6.
- [29] Lehmann V. Alkaline etching of macroporous silicon membranes. Porous semiconductors-science and technology, extended abstracts 5th international conference, Sitges, Spain, I4-01, 2006. p. 49–50.
- [30] Van Driel AF, Bret BPJ, Vanmaekelbergh D, Kelly JJ. Hot carrier luminescence during porous etching of GaP under high electric field conditions. *Surf Sci* 2003;529:197–203.
- [31] (a) Takizawa T, Arai S, Nakahara M. Fabrication of vertical and uniform-size porous InP structure by electrochemical anodization. *Jpn J Appl Phys* 1994;33:L643–5;
- (b) Kikuno E, Amiotti M, Takizawa T, Arai S. Anisotropic refractive index of porous InP fabricated by anodization of (111)A surface. *Jpn J Appl Phys* 1995;34:177–8.
- [\*\*32] Föll H, Langa S, Carstensen J, Christophersen M, Tiginyanu IM. Pores in III–V semiconductors. *Adv Mater* 2003;15(3):183–98.
- [33] Wloka J, Mueller K, Schmuki P. Pore morphology and self-organization effects during etching of n-type GaP(100) in bromide solutions. *Electrochem Solid-State Lett* 2005;8(12):B72–5.
- [34] Wloka J, Lockwood DJ, Schmuki P. High intensity and oscillatory electroluminescence observed during porous etching of GaP in HBr and HF electrolytes. *Chem Phys Lett* 2005;414:47–50.
- [35] (a) Ross FM, Oskam G, Searson PC, Macaulay JM, Liddle JA. Crystallographic aspects of pore formation in gallium arsenide and silicon. *Philos Mag A* 1997;75:525–39;
- (b) Oskam G, Natarajan A, Searson PC, Ross FM. The formation of porous GaAs in HF solutions. *Appl Surf Sci* 1997;119:160–8.
- [36] Langa S, Carstensen J, Christophersen M, Steen K, Frey S, Tiginyanu IM, et al. Uniform and nonuniform nucleation of pores during the anodization of Si, Ge, and III–V semiconductors. *J Electrochem Soc* 2005;152(8):C525–31.